Available online at www.sciencedirect.com
ScienceDirect
Physics Procedia 11 (2011) 15–18
Physics Procedia
www.elsevier.com/locate/procedia

Proceedings of APAC-SILICIDE 2010

Magnetoresistance characteristics of $Fe_3Si/CaF_2/Fe_3Si$ heterostructures grown on Si(111) by molecular beam epitaxy

K. Harada[a], K. S. Makabe[a], H. Akinaga[b] and T. Suemasu[a]

[a]Institute of Applied Physics, University of Tsukuba, Tsukuba, Ibaraki 305-8573, Japan

[b]Nanodevice Innovation Research Center, AIST, Tsukuba, Ibaraki 305-8569, Japan

Abstract

$Fe_3Si/CaF_2/Fe_3Si$ magnetic tunnel junctions (MTJs) have been investigated to demonstrate the tunnel magnetoresistance effects. We fabricated Fe_3Si(20 nm)/CaF_2(2 nm)/Fe_3Si(15 nm) heterostructures epitaxially on a Si(111) substrate by molecular beam epitaxy. The current-voltage characteristics for the MTJs measured at room temperature (RT) were well fitted to Simmons'

Keywords: Fe_3Si; CaF_2; MBE; MTJ; Magnetoresistance

1. Introduction

The tunnel magnetoresistance (TMR) effects are a phenomenon that occurs when electrons tunnel through ferromagnet-insulator-ferromagnet magnetic tunnel junction (MTJ) structures, leading to change in resistance depending on the relative orientation of magnetization with applied magnetic fields. MTJs have shown a large TMR effect, and thus the application of MTJs has been a key issue in the development of spintronics [1, 2]. We have focused on ferromagnetic silicide Fe_3Si and insulating CaF_2 aiming to realize resonant-tunneling-type spin source, where resonant tunneling and TMR effect are essential to be demonstrated. The lattice parameters of Fe_3Si and CaF_2 are 0.566 nm and 0.546 nm, respectively. Thus both Fe_3Si and CaF_2 are nearly lattice-matched to Si (0.543 nm), and Fe_3Si/CaF_2 heterostructures are grown epitaxially on Si(111) substrates [3]. Furthermore, Fe_3Si has a relatively high Curie temperature of approximately 570 ˚C [4]. Very recently, spin injection and detection in a Si channel through the Fe_3Si/Si Schottky-tunnel contacts has been reported [5]. We have developed a technique for epitaxial growth of Fe_3Si/CaF_2 heterostructures on Si(111) substrates by molecular beam epitaxy (MBE) [6-8]. The current density versus voltage (*J*-*V*) characteristics of the $Fe_3Si/CaF_2/Fe_3Si$ magnetic tunnel junctions (MTJs) measured at room temperature (RT) were well fitted to Simmons' equation, and the barrier height for electrons in the Fe_3Si to tunnel through the CaF_2 barrier was found to be approximately 2.5 eV [9]. Recently, we have realized clear negative differential resistance in $CaF_2/Fe_3Si/CaF_2$ ferromagnetic resonant tunnelling diodes at RT [10, 11]. In this paper, we report on the epitaxial growth of Fe_3Si(20 nm)/CaF_2(2 nm)/Fe_3Si(15 nm) MTJs on Si(111) substrates by MBE, and successfully demonstrated the TMR effect at RT.

1875-3892
doi:10.1016/j.phpro.2011.01.027

2. Experiments

The epitaxial Fe_3Si(20 nm)/CaF_2(2 nm)/Fe_3Si(15 nm) MTJ structures were fabricated by MBE onto a CaF_2(3 nm)/Si(111) substrate. First, a Si buffer layer (10 nm) was deposited on the Si(111) and was annealed at 1000 °C for 15 min to enhance crystallization and flatten the surface of the Si(111) substrates. Next, a CaF_2 buffer layer (3 nm) was deposited at 280 °C and was annealed at 300 °C to prevent the formation of secondary phases like FeSi. Fe_3Si(20 nm)/CaF_2(2 nm)/Fe_3Si(15 nm) heterostructures were grown on a CaF_2(3 nm)/Si(111) substrate. The growth temperatures were 140 and 280 °C for Fe_3Si and CaF_2, respectively, and each layer was annealed at 300 °C for 20 min. Finally, an Fe capping layer (5 nm) was deposited on the heterostructures at around 150 °C to change a coercive field, H_c , between the top Fe/Fe_3Si and the bottom Fe_3Si layers. The grown layers were processed into 600×20, 450×15, 300×10, 300×15 and 200×10 μm^2-area MTJs using a conventional photolithography, selective wet chemical etching, and lift-off processes. Fe_3Si was etched using HF: HNO_3: H_2O = 1: 2: 400 at 0 °C and CaF_2 was etched using H_2SO_4: H_2O = 1: 20 at 0 °C [9]. Ohmic contacts were formed on top of the MTJs using Au/Cr. The crystalline quality of grown layers was investigated by reflection high-energy electron diffraction (RHEED). The *J-V* characteristics and magnetic-field dependence of the resistance for the MTJs were measured by a standard two-probe method at RT.

3. Results & Discussion

Figure 1 shows RHEED patterns taken after each growth stage along the $[1\bar{1}0]$ azimuth of Si. The RHEED patterns clearly display sharp and fine streaky patterns, implying that the films with good crystalline quality together with a smooth surface was obtained from the 10-nm-thick Si buffer layer through the 20-nm-thick-Fe_3Si upper layer and the $Fe_3Si/CaF_2/Fe_3Si$ MTJ structures were epitaxially grown on the Si(111) substrate.

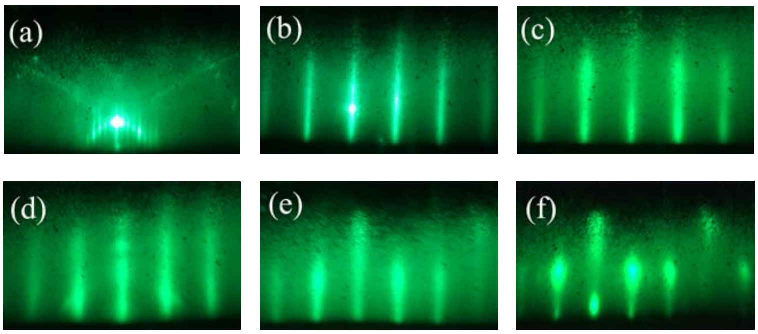

Fig. 1 RHEED patterns taken after each growth stage along $[1\bar{1}0]$ azimuth of Si: (a) Si buffer layer, (b) CaF_2 buffer layer, (c) Fe_3Si bottom ferromagnetic layer, (d) CaF_2 barrier layer (e) Fe_3Si upper ferromagnetic layer, and (f) Fe capping layer.

Figure 2 shows schematic cross section of MTJs processed by photolithography, wet etching, and lift-off processes. Figure 3 shows a typical example of *J-V* characteristics measured at RT with voltages applied between the top and the bottom Fe_3Si layers in the $Fe_3Si/CaF_2/Fe_3Si$ MTJ structures without external magnetic field. The positive bias voltage, V_+, is defined as that applied to the top Fe_3Si (20 nm) layer with respect to the bottom Fe_3Si (15 nm) layer as shown in Fig. 2. The data were well fitted to Simmons' equation as shown by the solid line [12]. The fitting yields the barrier height φ = 2.5 eV for electrons in the Fe_3Si layers to tunnel the CaF_2 barrier layers, which is the same as that previously reported [9], and the barrier thickness d = 1.26 nm. This result shows that the thickness of the CaF_2 barrier layer became substantially thinner than that designed, probably due to rough interface between the CaF_2 barrier layer and both top and bottom Fe_3Si ferromagnetic layers. Figure 4 shows the magnetoresistance characteristics measured for the 300×15 μm^2-area MTJs at RT under a bias voltage of 20 mV. The magnetic field H was applied parallel to the sample surface along the long axis of the MTJs. Magnetoresistance curve increases gradually at 0 Oe and reaches a maximum in the range of H = 100-200 Oe. The corresponding magnetoresistance ratio (MR = (R_{AP} – R_P)/R_P, P: parallel, AP: antiparallel) is approximately 0.28 % at RT. Dependence of TMR ratio on bias voltage is now under investigation.

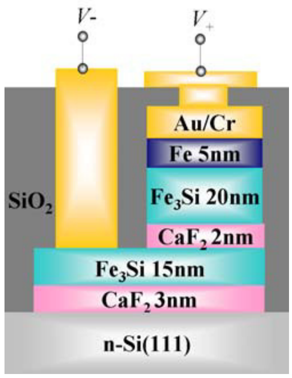

Fig. 2 Schematic cross section of fabricated MTJs.

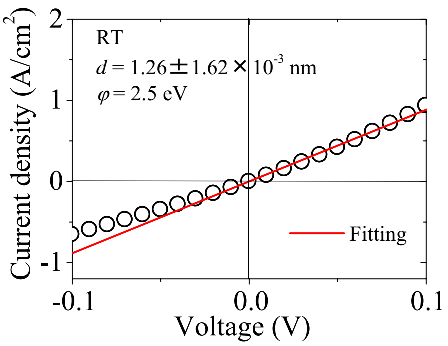

Fig. 4 Typical example of J-V characteristics for the fabricated MTJs at RT. The solid line shows the fitting.

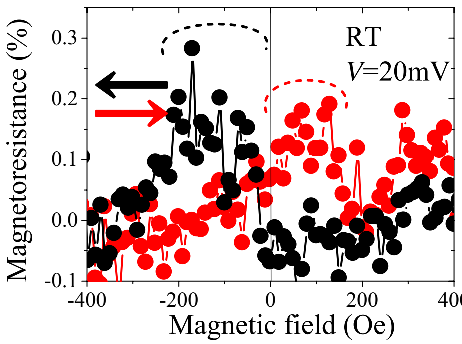

Fig. 3 Magnetic-field dependence of the resistance for the MTJs measured at RT under a bias of 20 mV.

4. Conclusion

The Fe_3Si (20 nm)/CaF_2 (2 nm)/Fe_3Si (15 nm) MTJ structure was fabricated epitaxially on Si(111) by MBE, and the electrical properties were measured. The J-V characteristics measured at RT were well fitted to the Simmons' equation, and the fitting yielded the barrier height φ = 2.5 eV and the barrier thickness d = 1.26 nm. We also obtained approximately 0.28 % TMR ratio at RT.

Acknowledgements

This work was supported in part by a Grant-in-Aid for Scientific Research in the Priority Area of "Creation and Control of Spin Current" (No. 19048029, MEXT). The authors also thank Prof. M. Isshiki and Dr. M. Uchikoshi of the Tohoku University for supplying us high-purity 5N Fe sources and Prof. E. Kita and Prof. H. Yanagihara, the University of Tsukuba, for their help in *J-V* and magnetoresistance measurements.

Refference

[1] T. Miyazaki and N. Tezuka, J. Magn. Magn. Mater. **139** (1995) L231.
[2] J. S. Moodera, Lisa R. Kinder, Terrilyn M. Wong and R. Meservey, Phys.Rev. Lett. **74** (1995) 3273.
[3] J. Kudrnovský, N. E. Christensen and O. K. Anderson, Phys. Rev.B **43** (1994) 5924.
[4] J. Waliszewski, L. Dobrzyński, A. Malinowski, D. Satuła, K. Szymański, W. Prandl, Th. Brückel and O. Schärpf, J. Magn. Magn. Mater. **132** (1994) 349.
[5] Y. Ando, K. Hamaya, K. Kasahara, Y. Kishi, K. Ueda, K. Sawano, T. Sadoh and Y. Miyao, Appl. Phys. Lett. **94** (2009) 182105.
[6] T. Sunohara, C. Li, Y. Ozawa, T. Suemasu and F. Hasegawa, Jpn. J. Appl. Phys. **44** (2005) L715.
[7] K. Kobayashi, T. Sunohara, M. Umada, H. Yanagihara, E. Kita and T. Suemasu, Thin Solid Films **508** (2006) 78.
[8] T. Harianto, K. Kobayashi, T. Suemasu and H. Akinaga, Jpn. J. Appl.Phys. **46** (2007) L904.
[9] T. Harianto, K. Sadakuni, H. Akinaga and T. Suemasu, Jpn. J. Appl. Phys. **47** (2008) 6310.
[10] K. Sadakuni, T. Harianto, H. Ainaga and T. Suemasu, Appl. Phys. Express **2** (2009) 063006.
[11] K. S. Makabe, M. Suzuno, K. Harada, H. Akinaga and T. Suemasu, Jpn. J. Appl. Phys. **49** (2010) 060212.
[12] J. G. Simmons, J. Appl. Phys. **34** (1963) 1793.